Author Manuscript
Faculty of Biology and Medicine Publication

This paper has been peer-reviewed but does not include the final publisher proof-corrections or journal pagination.

Published in final edited form as:

In vitro and in vivo ocular biocompatibility of electrospunpoly(ε-caprolactone) nanofibers

Gisele Rodrigues Da Silva Tadeu Henrique Lima Rodrigo Lambert Oréfice

Gabriella Maria Fernandes-Cunha Armando Silva-Cunha Min Zhao , Francine Behar-Cohen

Biocompatibility is a requirement for the development of nanofibers for ophthalmic applications. In this study, nanofibers were elaborated using poly(ε-caprolactone) via electrospinning. The ocular biocompati- bility of this material was investigated. MIO-M1 and ARPE-19 cell cultures were incubated with nanofi- bers and cellular responses were monitored by viability and morphology. The in vitro biocompatibility revealed that the nanofibers were not cytotoxic to the ocular cells. These cells exposed to the nanofibers proliferated and formed an organized monolayer. ARPE-19 and MIO-M1 cells were capable of expressing GFAP, respectively, demonstrating their functionality. Nanofibers were inserted into the vitreous cavity of the rat's eye for 10 days and the in vivo biocompatibility was investigated using Optical Coherence Tomography (OCT), histology and measuring the expression ofpro-inflammatory genes (IL-1b, TNF-a, VEGF and iNOS) (real-time PCR). The OCT and the histological analyzes exhibited the preserved architecture of the tissues of the eye. The biomaterial did not elicit an inflammatory reaction and pro- inflammatory cytokines were not expressed by the retinal cells, and the other posterior tissues of the eye. Results from the biocompatibility studies indicated that the nanofibers exhibited a high degree of cellular biocompatibility and short-term intraocular tolerance, indicating that they might be applied as drug carrier for ophthalmic use.

1. Introduction

Electrospinning is prevailing as the most convenient method for the fabrication of polymeric nanofibers. In the electrospinning pro- cess, the polymer solution is extruded from a nozzle to which ahigh electric voltage is applied (Reneker et al., 2000; Ishii et al., 2009). The extruded polymer solution is scattered by the repulsion of electrical charges accumulated at the surface of the solution. Then the droplets of the solution are elongated by the electrostatic force operating between droplet and substrate. The nanofiber is formed by the rapid evaporation of solvent from the droplet (Ishii et al., 2009).

Nanostructured materials exhibit distinctive and appealing characteristics compared to the bulk material due to small dimen- sions and large surface to volume ratio (Moriarty, 2001; Touseef et al., 2013). Additionally, the electrospun fibers present a high porosity and interconnected porous network. The characteristics of the nanofibers represent advantages of these biomaterials, which provide their applicability in a variety of biomedical fields.

Nanostructured scaffolds have been evaluated to study the adhesion, proliferation, and differentiation of different types of cells for functional tissue regeneration. These scaffolds should mimic the native extracellular matrix (EMC), providing not only the anchorage, growth, and functionalization of the cells, but also the efflux of metabolic products produced by those cells. Nowadays, the nanostructured cell supports have been applied in tissue engineering of bone (Shabani et al., 2014; Kocabey et al., 2013), cartilage (Buchtová et al., 2013; He et al., 2013), nerves (Subramanian et al., 2012; Du et al., 2014), blood vessels (Wang et al., 2013; Huang et al., 2013), among others. Besides the applica- tion as cellular carriers, polymeric nanofibers incorporated into principle actives have been investigated as delivery systems for releasing drugs over a long period of time for the treatment of dif- ferent pathologies.Anti-inflammatory agents (e.g., dexametha- sone) (Su et al., 2012), antibiotics (e.g., ampicillin, doxycycline) (Sohrabi et al., 2013; Chaturvedi et al., 2013), antitumor drugs (e.g., doxorubicin) Liu et al., 2014 represent some examples of therapeutic agents which were encapsulated and/or embedded into the nanometric fibers and were sustained released from them. The nanostructured drug delivery systems enable the increase of bioavailability of active agents of unfavorable physical and chemi- cal characteristics, assuring an effective therapy (Son et al., 2014).

In the field of the ophthalmology, the polymeric nanostructured materials have been evaluated as ocular cellular carrier for the treatment of severe pathologies, which can lead to impaired vision and/or blindness. For example, a 3D polyamide 6/12 nanofiber scaffold was applied as support for the growth and proliferation of mesenchymal and limbal stem cells for their transplantation and reconstitution of a mechanically damaged corneal surface in an experimental mouse model (Holan et al., 2013). The human cor- neal epithelial cell line was used to evaluate the biocompatibility of electrospun poly(ε-caprolactone) nanofibers. It was verified that the nanofibers provided not only a milieu supporting the corneal epithelial cells expansion, but also serve as a useful alternative car- rier for ocular surface tissue engineering and could be used as an alternative substrate to replace human amniotic membrane (HAM)Sharma et al., 2011.

Before the clinical application of the nanostructured materials in the reconstitution of damage tissues and organs, the biocom- patibility of these biomaterials must be extensively investigated. The biocompatibility studies of the potentially nanostructured scaffolds should involve laboratory and animal experiments which allows to determine their biological safety. Regarding the impor- tance of evaluating the biological safety of electrospun poly(ε- caprolactone) nanofibers, in this study, the in vitro and in vivo bio- compatibility of these nanostructured polymeric material was investigated to consider their suitability for ophthalmic applica- tions. The in vitro biocompatibility of the poly(ε-caprolactone) nanofibers was analyzed using Müller glial cells (MIO-M1) and retinal pigment epithelial cells(ARPE-19) cultures. The response of the ocular cells in direct contact with the nanofibers was

determined in terms of viability and capacity to proliferate and dif- ferentiate. The in vivo biocompatibility of the nanofibers was ana- lyzed after their implantation in the vitreous cavity of the rat's eye using the OCT, histology and the measurement

of the expression ofpro-inflammatory genes (real-time PCR). The ophthalmic applica- tion of the poly(ε-caprolactone) nanofibers depends on their intraocular biocompatibility, without eliciting inflammatory and immune responses or toxic reactions.

2. Materials and methods

2.1. Preparation of the poly(ε-caprolactone) nanofibers – electrospun nanofibers

Poly(ε-caprolactone) (PCL, MW 80,000–90,000 g/mol; Sigma Chemical Co., USA) solution [14.6% (w/v)] was prepared by dissolv- ing PCL pellets in a mixture of acetic acid and formic acid (1:1) (Sigma Aldrich, St. Louis, MO), under magnetic stirring for 3 h at room temperature. The clear solution was electrospunusing an electrospinning setup consisting of a dual polarity, high-voltage DC power supply unit (Gamma High Voltage Research, Ormond Beach, FL), a syringe pump (Arti Glass, CE, Italy), syringe (Dispovan, Faridabad, India), and a needle (24 G) with blunted tip. The positive terminal of the high-voltage supply was connected to the needle tip while the negative terminal was connected to a metallic collector plate; a voltage of +25 kV was maintained between them. Electrospun fibers were collected on coverslips kept over the metallic collector disc (8 cm of diameter). Flow rate was maintained at 3.6 mL/h and needle tip to collector distance was maintained at 9 cm.

2.2. Morphology and diameter of the PCL nanofibers

Morphology and diameter of the PCL nanofibers were analyzed by scanning electron microscopy (SEM) (JEOL JSM 5600, Japan) at an accelerating voltage of 15 kV. Samples for SEM were mounted on metal stubs and coated with gold using a sputter coater (JEOLJFC-1200 fine coater, Japan). Non-woven nanofiber mats were ana- lyzed with 50 individual measurements of nanofiber diameters taken from SEM micrographs using image analysis software (Image J, National Institutes of Health, USA). This was repeated for a single electrospun fiber mat fabricated under a single set of constant conditions to calculate the average nanofiber diameter and standard deviation.

2.3. In vitro biocompatibility study

2.3.1. ARPE-19 and Müller glial cell (MIO-M1 cell) cultures
ARPE-19 cells, an established but non-immortalized human RPE cell line, were graciously provided by Dr. Hjelmeland (University of California, Davis, CA) and were grown in a Dulbecco's modified eagles medium and Ham's F12 medium (DMEM/F12 Gibco BRL: Grand Island, NY) with 10% fetal bovine serum (FBS Gibco BRL: Grand Island, NY) in a 37 LC humidified atmosphere of 5% CO_2 and 95% air.

Müller glial cells (MIO-M1 cells), a spontaneously immortalized RMG cell line originated from human retina (Limb et al., 2002), were kindly provided by Dr. Astrid Limb (University College London, London, UK) and were grown in a Dulbecco's modified eagles medium/glutamax (DMEM/glutamaxGibco BRL: Grand Island, NY) with 10% fetal bovine serum (FBS Gibco BRL: Grand Island, NY), 0.4% gentamicin, and 0.1% amphotericin B at 37 LC in a humidified atmosphere of 5% CO_2 and 95% air.

The culture medium of both cells was refreshed every 2 days. Upon confluence, cells were rinsed with 2 mL of a 0.05% trypsin-EDTA (Gibco, Grand Island, NY) solution and incubated with 5 mL of trypsin-EDTA at 37 LC in a humidified atmosphere of 5% CO_2 and 95% air. Next, within 5–15 min, the trypsin enzyme activity was stopped by the addition of 5 mL of complete growth medium and centrifuged for 5 min at 1500 rpm. The supernatant was discarded, while the cells were resuspended in 13 mL of fresh medium and seeded onto culture flasks for further propagation and subsequent passages.

2.3.2. ARPE-19 and MIO-M1 cell cultures in contact with PCL nanofibers
The PCL nanofibers were cut into round pieces (4.5 mm in diameter, average weight of 0.12 mg ± 0.09 and n = 10), and disin- fected by exposure to UV light for 90 min on each side prior to cell culture. ARPE-19 and MIO-M1 cells were plated in contact of the 10^3 cells/well.

2.3.3.ARPE-19 and MIO-M1 cell proliferation in contact with PCL nanofibers (nuclear count)

After 1, 2, 5 and 10 days in the culture, the medium was aspi- rated, and the ARPE-19 and MIO-M1 cells in contact with PCL nanofibers and control TCPS were rinsed with phosphate-bufferedsaline (PBS) and fixed in paraformaldehyde 4% (v/v) (Merck Eurolab, Fontelay Sous-Bois, France) for 15 min. Next, fixed cells were rinsed again with PBS for 5 min and immersed in PBS con- taining 0.3% (v/v) Triton X-100 (Sigma- Aldrich) for 15 min. After rising in PBS for 5 min, the nuclei were stained with 4_0,6-diami-dino-2-phenylindole (DAPI) (Sigma-Aldrich) in PBS (1:1250) for 5 min at room temperature. Finally, the cells were washed five times at 5 min intervals with PBS and one time with water, mounted in Gel Mount

(Biomeda, Burlingame, CA) and viewed using an Olympus IX70 fluorescent microscope attached to a digi- tal camera (Olympus DP70). Five fields were photographed per PCL

nanofibers and control TCPS (total of 15 fields per surface per time- point). The nuclei were counted for each field of view (0.59 mm$_2$). The average number of nuclei on the control surface was set as 100%, while the average number of nuclei ± standard deviation in contact with PCL nanofibers was obtained as a percentage of the control. Data were presented as a histogram.

2.3.4.Cytotoxicity of the PCL nanofibers

After 1, 2, 5 and 10 days in the culture, the medium was aspi- rated, and the ARPE-19 and MIO-M1 cells in contact with PCL nanofibers and control TCPS were rinsed with phosphate-bufferedsaline (PBS). The ARPE-19 and MIO-M1 cells were incubated with 150 İL of 3-[4,5-dimethylthiazol-2-yl]-2,5-diphenyltertrazoliumbromide (MTT) (1 mg/mL in PBS) (Sigma Chemical, Saint Louis, CO). After 3 h of incubation, the cells were lysed with 100 İL of iso- propanol, and absorbance values were measured at 570 nm versus 630 nm using a microplate reader (BioRad, San Diego, CA). The mean absorbance on the control surface was set as 100%, while the mean absorbance ± standard deviation in contact with PCL nanofibers was obtained as a percentage of the control. Data were presented as a histogram.

2.3.5. Morphology of the ARPE-19 and MIO-M1 cells – Immunofluorescence

At 10 days of culture, the ARPE-19 and MIO-M1 cells in contact with PCL nanofibers and control TCPS were submitted to the same procedure described for the proliferation study. After nuclei stain- ing with DAPI, F-actin fibers were labeled with Phalloidin FITC(Sigma-Aldrich) in PBS (1:250) for 30 min at room temperature. Cells were then rinsed, mounted, and viewed using Olympus

IX70 fluorescent microscope attached to a digital camera (Olympus DP70).

At 10 days of culture, for the labelling of occludin tight junc- tions, the ARPE-19 cells grown in contact with PCL nanofibers and control TCPS were fixed with p-formaldehyde 4% (v/v) for 30 min at room temperature. The fixed cells were incubated with PBS containing Triton X-1000.1% (v/v) for 30 min. This was fol- lowed by incubation with the rabbit anti-Occludin (Zymed Laboratories, South San Francisco, CA) in PBS containing Triton X- 1000.1% (v/v) (1:100) for 60 min. The cells were rinsed twice with PBS for 10 min and incubated with an Alexa Fluor 488 goat anti- rabbit secondary antibody (Molecular Probes) in PBS (1:250) for 60 min in the dark. Finally, cells were rinsed, mounted, and viewed using Olympus IX70 fluorescent microscope attached to a digital camera (Olympus DP70).

At 10 days of culture, for the labelling of glial fibrillary acidic protein (GFAP), the MIO-M1 cells grown in contact with PCL nano- fibers and control TCPS were fixed with p-formaldehyde 4% (v/v) for 30 min at room temperature. The fixed cells were incubated with PBS containing Triton X-100 0.1% (v/v) for 30 min. This was followed by incubation with polyclonal rabbit antibody against GFAP (1:100) (Dako, Trappes, France) at room temperature for 3 h. After washing with PBS, an Alexa Fluor 488-conjugated goat anti-rabbit IgG (1:100) (Molecular Probes, Leiden, The Netherlands) was applied for 60 min in the dark. Finally, the nuclei were stained with DAPI (Sigma-Aldrich)in PBS (1:1250) for 5 min at room temperature. Then, the cells were rinsed five times, mounted, and viewed using Olympus IX70 fluorescent microscope attached to a digital camera (Olympus DP70).

2.4. In vivo biocompatibility study

2.4.1. Animals

Female Lewis rats (8–12 weeks old; Janvier, Le Genest-Saint-Isle, France) were kept in pathogen free conditions with food and water ad libitum and housed in a 12-h light/12-h dark cycle. The animals were divided into two groups: (1) rats without PCL nano- fibers (control group); (2) rats receiving PCL nanofibers into the vitreous cavity. For each experimental series, the number of ani- mals was indicated in the figure legends. All experiments were per- formed in accordance with the European Community's Council Directive 86/609/EEC and approved by ethical committees of the Université René Descartes.

2.4.2. Insertion of the PCL nanofibers into the vitreous cavity

PCL nanofibers of 1 mm of ray were sterilized as previously described. The animals were anaesthetized with an intraperitoneal injection of xylazine (20 mg/kg) and ketamine (80 mg/kg). The left pupil was dilated with tropicamide eye drops (Johnson & Johnson Vision Care, USA). To implant the PCL nanofibers into the vitreous cavity, the conjunctiva was dissected at the limbus in the temporo- superior quadrant and a 1 mm scleratomy was performed at 2 mm posterior to the limbus. The PCL nanofibers were introduced into the vitreous cavity through a trans-choroid way.

2.4.3. Optical Coherence Tomography (OCT)

In vivo assessment of rat's choroid and retina was performed on anesthetized animals using spectral domain Optical Coherence Tomography (OCT) (SD-OCT; Spectralis device) adapted for small animal eyes (Fischer et al., 2009). Pupils were dilated with 5% tropicamide drops (Théa). Scans were taken after 10 days of inser- tion of the PCL nanofibers into the

vitreous cavity of rat's eye. The rats of the control group were submitted to the same OCT evalua- tion. The temporal, nasal, and superior quadrants of the retina were analyzed, using the optic nerve head and the retina vessels as landmarks. Each 2-dimensional B-scan recorded at 30L field of view consisted of 1,536 A-scans with an optical resolution reaching 3.5 İm, and the enhanced depth imaging option was used to evalu- ate the choroid and retina. Retinal layers and choroid thickness was measured manually every 100 İm from the peripheral to the posterior pole. For analysis, the retina and choroid was divided into 3 zones: periphery, middle, and posterior pole. In the middle sec- tion, 3-4individual measurements were performed per rat (n = 5 per group).

2.4.4. Morphology

Animals of both groups were sacrificed using a lethal dose of pentobarbital (100 mg/kg – intraperitoneal injection) at 10 days of the experiment. Enucleated eyes were fixed in glutaraldehyde 2.5% (v/v) in cacodylate buffer (0.1 mol/L, pH 7.4). After 5 h of fixa- tion, the eyes were dehydrated in a graded alcohol series (50%, 70%, 95%, and 100%) and embedded in epoxy resin. Semi thin sections (1 İm) were cut using an ultramicrotome (Reichert Ultracut E, Leica, Wetzlar, Germany) and stained with toluidine blue. The mor- phology was examined under a light microscope (Olympus IX70) attached to a digital camera. Retinal layers and choroid thickness was measured manually every 100 İm from the peripheral to the posterior pole. For analysis, the retina and choroid was divided into 3 zones: periphery, middle, and posterior pole. In the middle sec- tion, 3–4 individual measurements were performed per rat (n = 3 per group).

2.4.5. Immunofluorescence

Enucleated eyes were fixed in paraformaldehyde 4% (v/v) for 30 min and incubated with a graded series of sucrose before being snap frozen in Tissue-Tek OCT-compound (Bayer Diagnostics, Puteaux, France). Ten micrometer cryostat sections of rat eyes were obtained. Unspecific binding sites were blocked with 5% nor- mal goat serum for 1 h. The sections were then incubated with pri- mary antibody mouse rabbit anti-ionized calcium binding adaptormolecule-1 (anti-IBA-1, 1:400, Wako, Richmond, USA). After wash- ing, slides were stained for 5 min with DAPI and washed again. The second antibodies was Alexa Fluor 488-coupled goat anti-rabbit IgG (1:200, Invitrogen). Negative controls were performed by omission of primary antibody. Four eyes from 4 rats per group and 4 sections per eye were analyzed.

2.4.6. Reverse transcription and real-time PCR

Animals of both groups were sacrificed using a lethal dose of pentobarbital (100 mg/kg – intraperitoneal injection) at 10 days of the experiment. Enucleated eyes were dissected at the level of the limbus and lens removed. The retina and posterior part of the eye were frozen and stored at 80 LC for preservation. Total RNA was isolated from the retina and posterior part of the eye using RNeasy Mini Kit (Qiagen, Courtaboeuf, France). First-strand cDNA was synthesized after DNase I (Qiagen) treatment using ran- dom primers (Invitrogen) and superscript II reverse transcriptase (Invitrogen). Transcript levels of TNF-α, IL1β, VEGF and iNOS were analyzed by real-time PCR performed in 7500 Real-Time PCR System (Applied Biosystems, Foster City, CA, USA) with either TaqMan (Applied Biosystems) or SYBR Green (Invitrogen) detec- tion. The 18S gene was used as internal control. Table 1 shows the references or sequences of primers used for both techniques.Delta-delta cycle threshold calculation (Ouvrard-Pascaud et al., 2005) was used for relative quantification of results.

2.5. Statistical analysis

Results were expressed as mean ± standard deviation. Data were tested for normality and investigated for statistical signifi- cance using the Student´s t test and one-way analysis of variance (ANOVA), where appropriate. A P-value of less than 0.05 was con- sidered significant.

Table 1
Real-time PCR primers and probes.

Gene	TaqMan probe reference or SYBR Green primer	
18S Human	Hs99999901_s1[a]	
18S Human and rat	Sense	5′-TGCAATTATTCCCCATGAACG-3′
	Antisense	5′-GCTTATGACCCGCACTTACTGG-3
HPRT1	Rn01527840_m1	
HPRT1	Sense	5′-GCGAAAGTGGAAAAGCCAAGT-3′
	Antisense	5′-GCCACATCAACAGGACTCTTGTAG-3′
	Rn01525859-	
TNF-α		g1
IL1b	Rn00676333_g1	
iNOS	Sense	5′-CTC GG A GGT CCA CCT CAC TGT-3′
	Antisense	5′-GGT TAT TGA TCC AAG TGC TGC-3′

[a] Patent of TaqMan . Sequence is not available.

3. Results

3.1. Morphology and diameter of the PCL nanofibers

Fig. 1 represented the SEM image of the PCL nanofibers. The electrospinning process provided the deposition of interconnected fibers. This nanometric three-dimensional network presented high porosity. Finally, the average fiber diameter was 130 ± 62 nm.

3.2. In vitro biocompatibility study

3.2.1. ARPE-19 and MIO-M1 cell proliferation in contact with PCL nanofibers (nuclear count)

The proliferation of ARPE-19 cells in contact with PCL nanofi- bers and control TCPS was expressed as percentage of cells in com- parison with the day-1. On days 2, 5 and 10, the percentage of RPE cells in contact with PCL nanofibers and control TCPS increased sig- nificantly (Fig. 2A), indicating the proliferative capacity of these ocular cells. Additionally, the number of MIO-M1 cells in the pres- ence of the PCL nanofibers and in the control TCPS on days 2, 5 and 10 progressively increased (Fig. 2B), demonstrating the growth of these neuroretina cells. Although the number of cells was greater in the control TCPS for all time intervals, the statistical analysis (one-way ANOVA) showed that there was no significant differ- ences in cell proliferation in contact with PCL nanofibers and con- trol TCPS ($p < 0.05$) after 2, 5, and 10 days of in vitro culture.
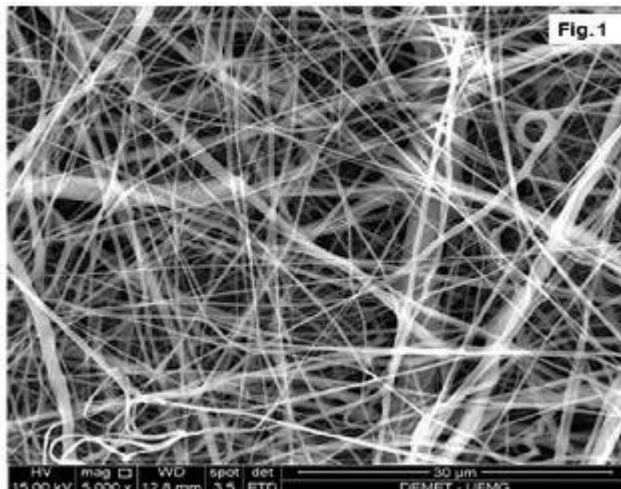

Fig. 1. SEM photomicrograph – morphology of electrospun PCL nanofibers. 5000magnification. Scale bar – 30 lm.
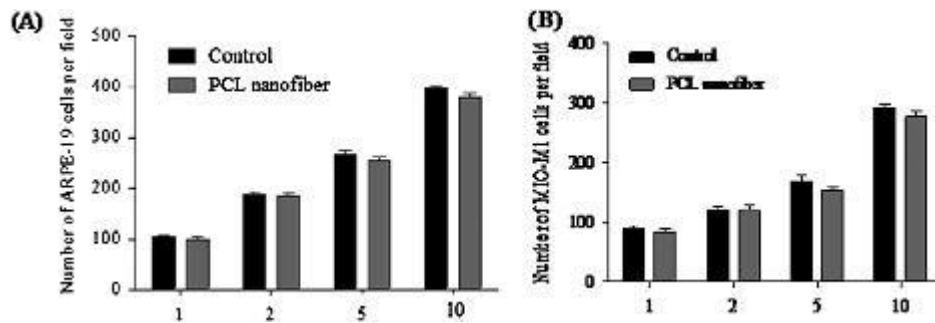
Fig. 2. Proliferation kinetics of (A) ARPE-19 cells and (B) MIO-M1 cells cultured in direct contact with PCL nanofibers and control TCPS at 1, 2, 5 and 10 days of incubation. Data were expressed as mean number of nuclei ± standard deviation for each time-point (n = 10 per group, per day) (p < 0.05).

3.2.2. Cytotoxicity of the PCL nanofibers

Fig. 3 demonstrated the viability of ARPE-19 and MIO-M1cellscultured in contact with PCL nanofibers and control medium. The viability of the ocular cells was evaluated at 2, 5 and 10 days of incubation. Accordingly, the polymeric nanofiber and its degrada- tion products showed to be no toxic to RPE and MIO-M1 cells, since there were no significant differences on the viabilities of these ocu- lar cells in all medium (control and treated groups) (one-way ANOVA, p < 0.05). It was suggested that the PCL nanofiber and its possibleby-products did not present cytotoxic effects against ARPE-19 andMIO-M1 cells in vitro cultured.

3.2.3. Morphology of the ARPE-19 and MIO-M1 cells – Immunofluorescence

The morphology of the ARPE-19 and MIO-M1 cells was evalu- ated after 10 days of seeding in direct contact with the PCL nanofi- bers. The RPE cells (Fig. 4A) reached a confluent level and a high cell density was evidenced. Staining of actin fibers in the cytoskele- ton revealed a highly interconnected cell network, since the actin filaments were running parallel to one another through the upper part of the cytoplasm, and being inserted into the intercellular membrane of adjacent cells, thus providing a connection between them (Silva et al., 2011). Staining of cell nuclei indicated that they were centrally located and did not appear to overlap, suggesting a monolayer formation. Additionally, these ARPE-19 cells were cap- able of expressing the occludin (Fig. 4B), demonstrating their func- tionality. The occludin is a transmembrane tight junction protein involved in theblood-retinal barrier. This barrier prevents the dif- fusion of solutes through the neuroretina (Tsukita et al., 1991). Therefore, the PCL nanofibers did not downregulate the expression of this tight junction protein.

The MIO-M1 cells, cultured in the presence of the PCL nanofi- bers, showed typical morphological features. The Müller glial cells (Fig. 4C) reached confluence on the glass coverslips. These retinal cells expressed the microfilament actin, revealing the existence of elongated and radially oriented cells. The nuclei were ellipsoid and highly centralized. The MIO-M1 cells demonstrated their abil- ity to express the glial fibrillary acidic protein (GFAP) (Fig. 4D) similarly to the control cells. GFAP is a ubiquitous marker for glia and an important cytoskeletal component determining cell mor- phology(Shao-Fen et al., 2013). Finally, the PCL nanofibers did not interfere in the expression of the GFAP; therefore the bio- material did not promote detectable modifications in the MIO- M1 phenotype.

3.3. In vivo biocompatibility study

3.3.1. Optical Coherence Tomography (OCT)

The in vivo OCT images demonstrated that the PCL nanofiber and possible by-products of the PCL in the vitreous cavity of the
rat's eye did not affected the integrity of the choroid and retinal layers when compared to the control group, which did not receive the polymeric nanofibers (Fig. 5A and B, respectively). Moreover, the choroid thickness of both groups of animals was measured, and there was no statistically significant difference between the thickness of this ocular structure (t-Student, p < 0.05) (Fig. 5C). The retinal layers thickness in the middle pole was also measured and the significant difference between animals receiving PCL nano- fibers and control was not detected (t-Student, p < 0.05) (Fig. 5C). These quantitative data corroborated with the qualitative observa- tions using in vivo OCT; and confirmed that the nanobiomaterials did not interfere in the choroid and retinal architectures during the follow-upperiod of intravitreal implantation. The OCT images also demonstrated that the vitreous cavity did not present hemor- rhages or abnormalities. Finally, the short-term in vivo biocompati- bility of the PCL nanofibers and their degradation products could be visualized using the OCT scan of the tissues of the posterior seg- ment of the eye.

3.3.2. Morphology

PCL nanofibers implanted in the vitreous cavity of the rat's eye were well tolerated, considering that no clinical evidence of immediate or delayed intraocular inflammation could be observed (Fig. 6A). Histological examination of the posterior and anterior segments of the eye showed that the architecture of the ocular tis- sues was completely preserved after 10 days of

intravitreal implantation of the PCL nanofibers (Fig. 6B) when compared to the architecture of the segments of the rats of the control group (Fig. 6C). No infiltration of inflammatory cells was observed on any of the ocular sections. Moreover, the choroid thickness of both groups of animals was measured and there was no statistically sig- nificant difference between the thickness of this ocular structure (t-Student, $p < 0.05$) (Fig. 6D). The retinal layers thickness in the middle pole was also measured and the significant difference between animals receiving PCL nanofibers and control was not detected (t-Student, $p < 0.05$) (Fig. 6D). Finally, the histological examination corroborated with data obtained in the OCT scans, providing information of the in vivo biocompatibility of the PCL nanofibers and the possible degradation products from the poly- meric chains.

3.3.3. Immunofluorescence

The microglia and macrophage activation was evaluated using theanti-ionized calcium binding adaptor molecule 1 (IBA-1) after 10 days of insertion of the PCL nanofibers in the vitreous cavity of the rat's eye. Accordingly, the number of activated microglia and macrophage was extremely low in the retina in the presence of the nanometric fibers and in the control group (Fig. 7A and B). This result indicated the excellent biocompatibility of the nano- metric fibers since activated microglial cells and recruited macrophages are directly implicated in retinal degeneration, probably through the secretion of pro-inflammatory mediators and cytotoxic factors, such as TNF-a, IL-1b, nitric oxide, among others (Rutar et al., 2012). Moreover, the number of activated macrophage and microglia in the ciliary body of the eyes of the ani- mals receiving PCL nanofibers was insignificant (Fig. 7C and D), suggesting that the IBA-1 stained only the resident cells; and the nanomaterial did not elicit an inflammatory response in the ante- rior segment of the eye.
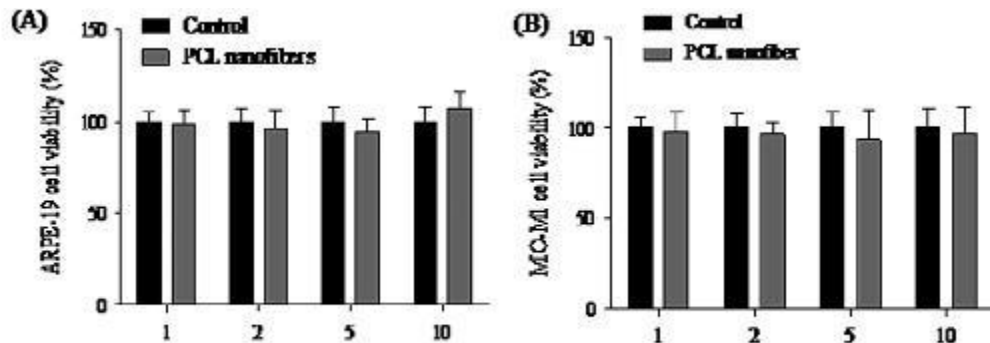

Fig. 3. Viability of (A) ARPE-19 and (B) MIO-M1 cells cultured in direct contact with PCL nanofibers and control medium, at 1, 2, 5 and 10 days of incubation (n = 10 for each PUD per group, per day) ($p < 0.05$). The viability of the ocular cells in contact with PCL nanofibers was relative to the control, fixed at 100%.
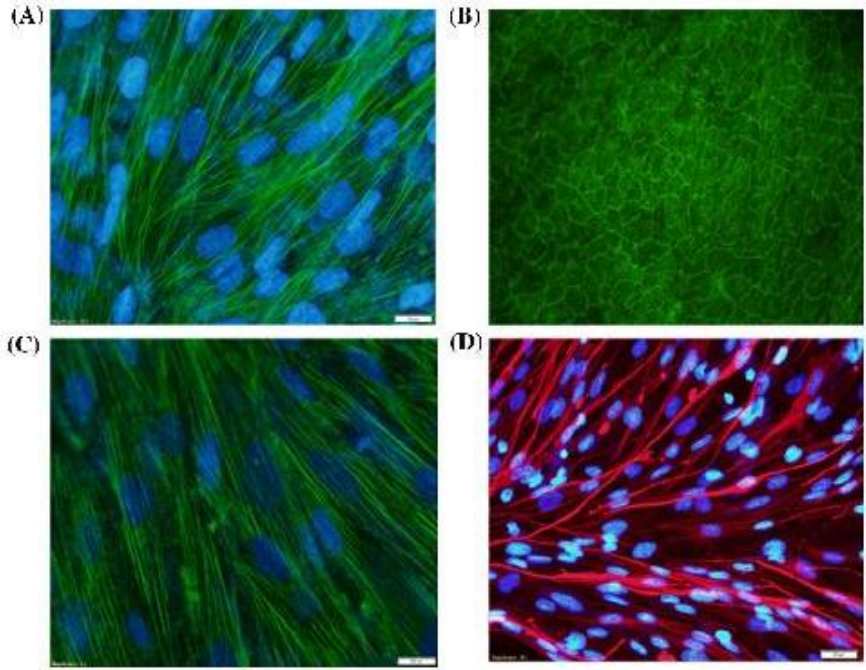
Fig. 4.
Micrographs of ARPE-19 and MIO-M1 cells in contact with PCL nanofibers for 10 days. (A) F-actin (green) and nuclei (blue) of ARPE-19 cells stained with Phalloidin FITC and DAPI after 10 days of culture (80). (B) Intercellular tight junctions (occludin) (green) between adjacent ARPE-19 cells (80). (C) F-actin and nuclei ofMIO-M1 cells stained with Phalloidin FITC and DAPI after 10 days of culture (40). (D) GFAP (red) expressed by Müller glial cells (40). (For interpretation of the references to colour in this figure legend, the reader is referred to the web version of this article.)
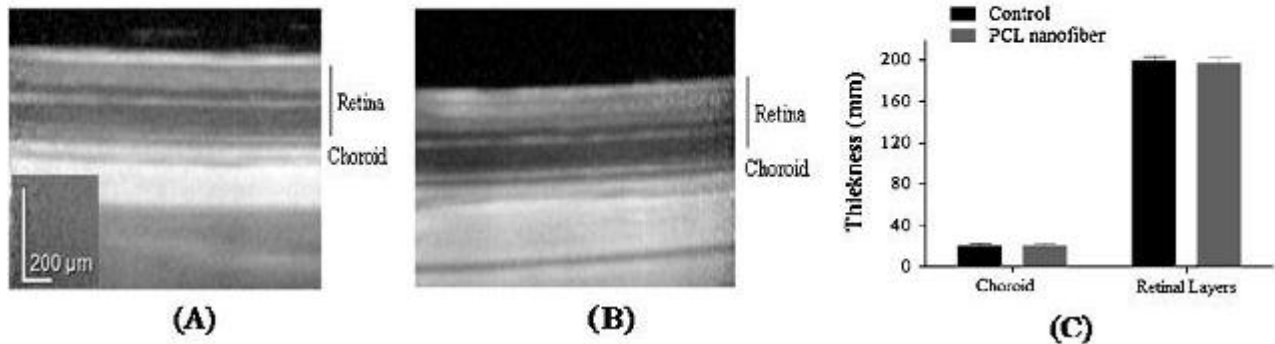

Fig. 5. In vivo OCT scan of the choroid and retinal layers of the rat's eye which received PCL nanofibers (A) and the animals of the control group (without polymeric implants)
(B). Choroid and retinal layers thickness of the animals of both groups (p < 0.05) (n = 6 per group) (C). Scale bar – 200 lm.
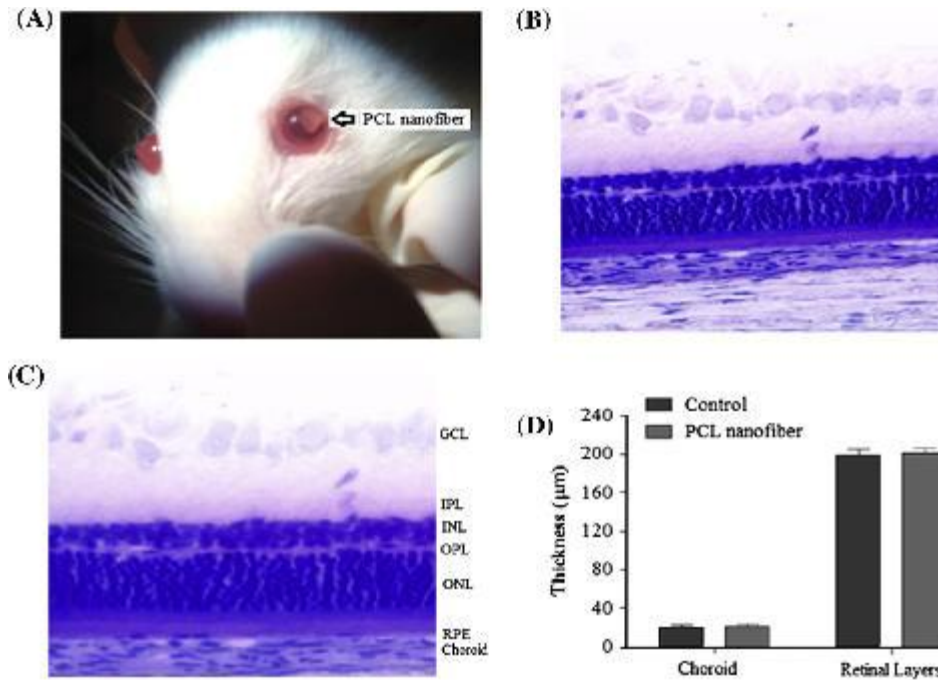
Fig. 6. Well tolerated PCL nanofiber in the vitreous cavity of the rat's eye after 10 days of implantation (A). Toluidine blue stained histological section on postoperative day 10 with PCL nanofibers within the vitreous cavity of the rat's eye (B) and the animals of the control group (without polymeric nanofibers) (C) (40). Choroid and retinal layers thickness of the animals of both groups were not statistically different (p < 0.05) (D) (n = 3 per group). Retinal layers: RPE – retinal pigment epithelium; ONL – outer nuclear layer; OPL – outer plexiform layer; INL – inner nuclear layer; IPL – inner plexiform layer; GCL – ganglion cell layer. (For interpretation of the references to colour in this figure legend, the reader is referred to the web version of this article.)
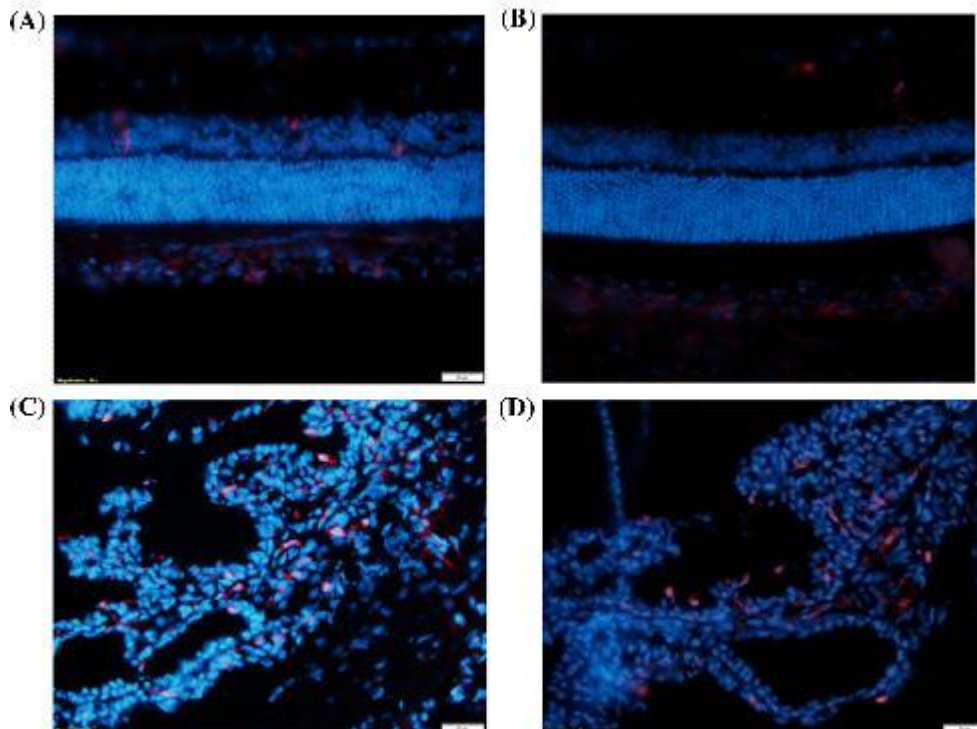

Fig. 7. Immunofluorescence detection of IBA-1 activated microglia and macrophage (red) in the retina of rat's eye after receiving PCL nanofibers for 10 days (A) and in the eyes of the control group (without polymeric nanofibers) (B). The nuclei of retinal cells was stained with DAPI. IBA-1 resident macrophage (red) in the ciliary body of the anterior segment of the rat's eye in the presence of polymeric nanofibers (C) and in the eyes of the control

group (D). The nuclei of ciliary body cells was stained with DAPI (40). Scale bar – 20 lm. (For interpretation of the references to colour in this figure legend, the reader is referred to the web version of this article.)

3.3.4. Reverse transcription and real-time PCR

The expression of some pro-inflammatory genes (IL-1b, TNF-a,VEGF and iNOS) by retinal cells and cells of the posterior part of the eye in direct contact with the PCL nanofibers was measured to verify the capacity of these nanostructured materials to induce an inflammatory response. Accordingly, the polymeric nanofibers did not significantly stimulate the expression of the pro-in- flammatory mediators compared to the production of them by the retinal cells and posterior ocular cells in the control group (Fig. 8) (t-Student, $p < 0.05$). Therefore; the PCR results suggested that the PCL nanofibers did not change the pattern of expression of some importantpro-inflammatory genes by the ocular cells. Finally, data obtained from IBA-1 stained were in concordance with the quantitative results obtained from RT-PCR.

4. Discussion

In this study, PCL nanofibers were elaborated based on the elec- trospinning technique. The electrospinning configuration, the
operational conditions (applied electric field of +25/0 kV; needle-to-collector distance equivalent of 9 cm; flow rate of 3.6 mL/h) and the solubilization of the PCL in a mixture of acetic acid and for- mic acid (1:1) yield the existence of ultrafine polymeric fibers. The high dielectric constant of the formic acid (e = 57.5) along with the polyelectrolyte character of the formic acid and acetic acid were responsible for a high electrical conductivity, leading to a greater tensile force, which could induce to an increase in the stretching and splitting of the jet, resulting in a thinner fiber and broader diameter distribution of the PCL nanofibers (Meng et al., 2010).

The PCL nanofiber was synthetized aiming the ophthalmic applications. However, the biocompatibility of this nanostructured material must be investigated prior to its clinical application. Besides the PCL is a biodegradable and biocompatible polymer, the possibility of the existence of solvent residues in the ultrafine mats could be toxic to the ocular tissues resulting in the fail in the ophthalmic use of these polymeric nanofibers. Any minimum level of toxicity of the solvent residues would be enough to cause a severe inflammatory response in the posterior segment of the eye, and consequently, to disturb the integrity of the neural retina and other tissues of the eye. The disruption of the neural retina eventually results in reduction of the visual acuity and/or blind- ness. Therefore, low levels of toxicity would be enough to lower our expectations regarding using the developed PCL nanofibers in ophthalmic applications.

The in vitro biocompatibility of the nanostructured materials was demonstrated using MIO-M1 and ARPE-19 cells. The viability of these cells in direct contact with the PLC nanofibers indicated a high survival rate over a period of 10 days in in vitro culture con- ditions. It supports the idea that PCL nanofiber and its by- products were non-toxic and biocompatible. Furthermore, the cells pro- liferated and differentiated in the presence of the ultrafine materi- als. TheARPE-19 cells were capable of expressing occludin, suggesting the presence of tight junctions among them. The obtained result indicated that RPE cells presented cell-cell interac- tions, which is essential for the formation of a functional endothe- lial monolayer (Silva et al., 2011). The RPE must adopt a tight epithelial monolayer phenotype, which acts as a blood-retinal bar- rier (Lu et al., 2007). The MIO-M1cells also demonstrated their functionality in contact with PCL nanofibers, since their endochy- lema contained large number of actin filaments and they produced GFAP similarly to the control cells (without contact with the nano- fibers). The similar pattern of GFAP production by the MIO-M1 cells of both groups indicated that cells were not under stress, once the up-regulation of GFAP is an early event under retinal stress conditions (Bringmann et al., 2009).
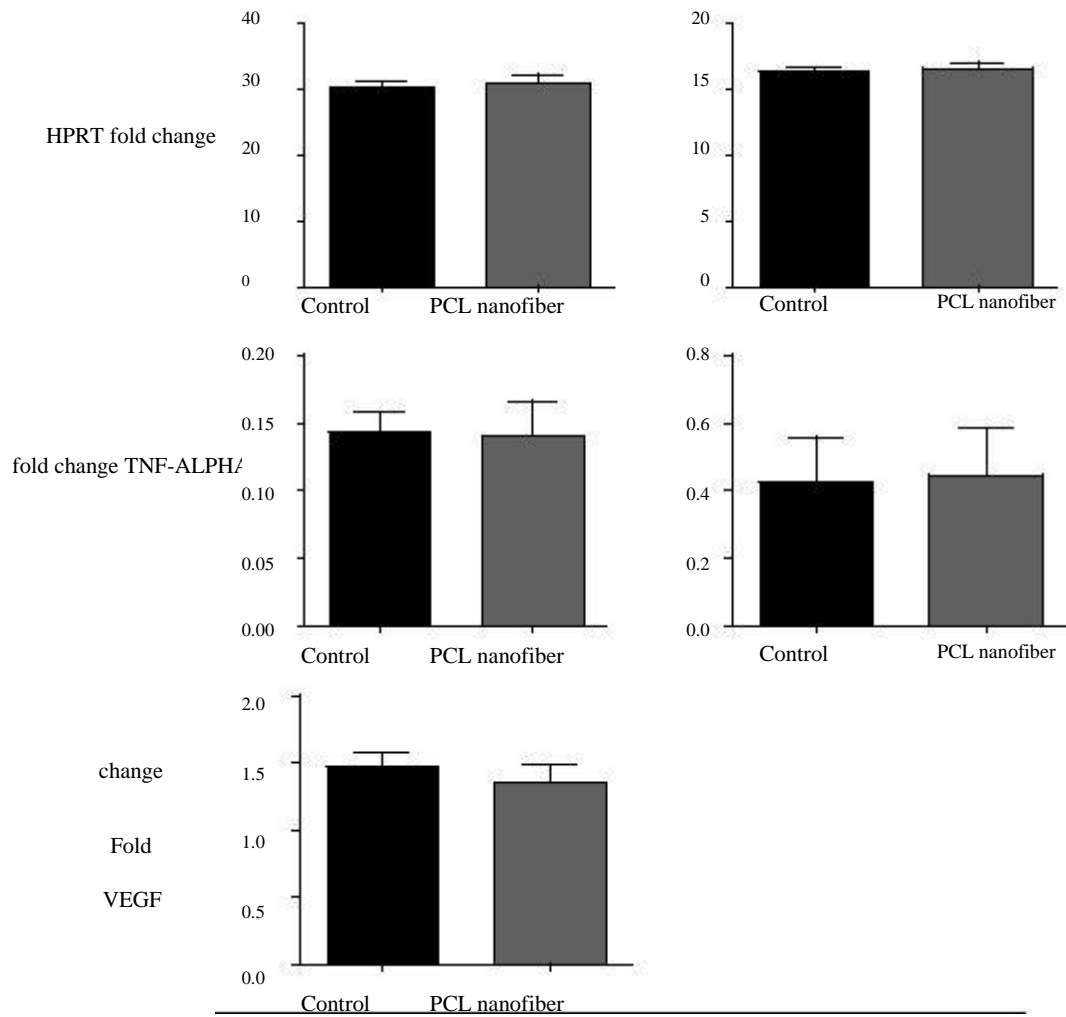
Fig. 8. Real-time PCR of pro-inflammatory genes (IL-1b, TNF-a, VEGF and iNOS) produced by retinal cells and cells of the posterior part of the eye in direct contact with the PCL nanofibers and in the control group.
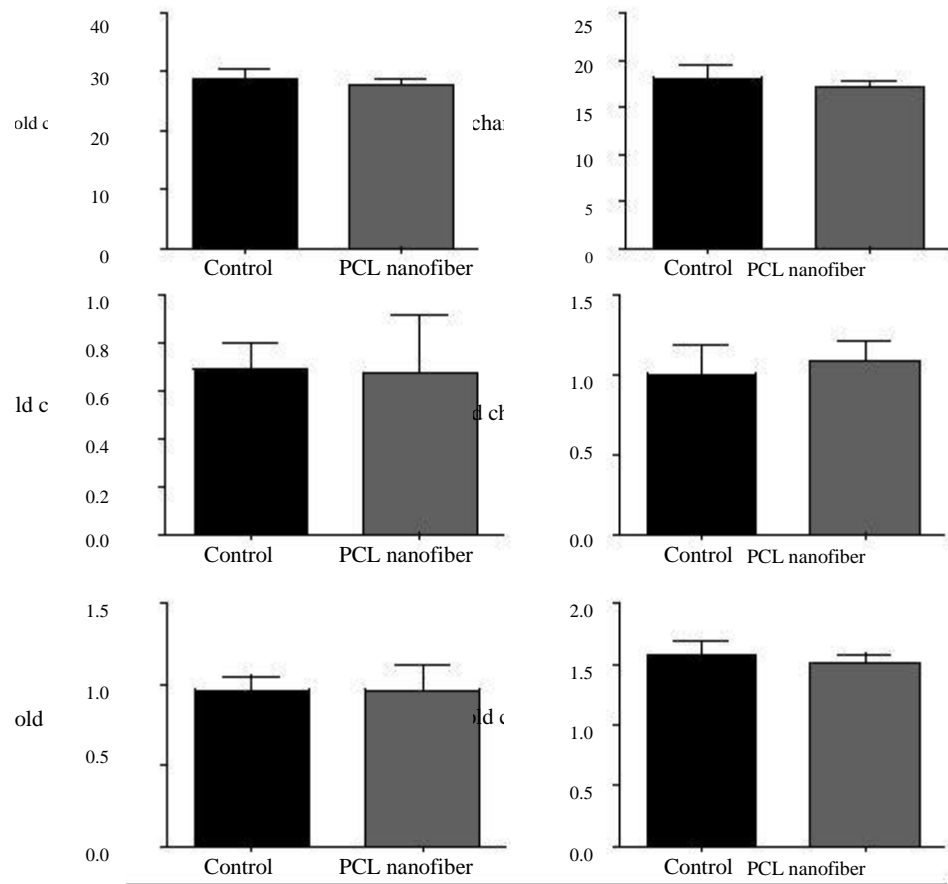
Fig. 8 (continued)

The in vitro biocompatibility studies demonstrated several encouraging findings about the electrospun PCL nanofibers in the presence of retinal cells. The obtained results were similar of those previously reported by Sharma and co-workers (Sharma et al., 2011), who showed the biocompatibility of electrospun PCL nano- fibers in contact with human limbal epithelial cell line (LEC). The fabricated nanofibers were able to support the attachment and proliferation of viable LEC line. It was hypothesized that the trans- plantation of ex-vivo expanded LEC could be a promising proce- dure to treat the dysfunction or loss of corneal limbal epithelial cells. On the other hand, in our work; the produced PCL nanofibers were not capable of supporting ARPE-19 and MIO-M1 cells, which areanchorage-dependent cells. Our PCL nanofiber presented a 3D pattern, which closely mimics the extracellular matrix environ- ment of the tissue; and it is required for successful retinal cell adhesion and subsequent transplantation (Sharma et al., 2011); however, besides this favorable characteristic, they did not pro- mote the adhesion of the ARPE-19 and MIO-M1 cells probably due to the high hydrophobicity of the PCL. It was previously docu- mented that the hydrophobicity of the PCL limits the adhesion of cells (Kim and Cho, 2009). The strategies to induce the cell adhe- sion and proliferation onto the surface of the PCL nanofibers could be: (1) the incorporation of cell-recognition domains such as bioac- tive proteins. For example, the collagen exposed on the surface of the nanofibers interacts with fibronectin, a glycoprotein, which binds the collagen to the integrin receptor on cell membranes, pro- moting cell adhesion onto the surface of the PCL nanofibers (Schnell et al., 2007); (2) the enhancement of the hydrophilicity of the surface using plasma treatment. Accordingly, plasma surface treatment of a polymeric matrix with N_2, O_2 and NH_3 makes the surface of the matrix more hydrophilic and more bioadhesive (Bakhshandeh et al., 2011); (3) the association of the PCL with a hydrophilic polymer forming a blended nanostructured biomateri- al. Polymer blending is one of the most effective methods for pro- viding new and desirable biocomposite for particular applications(Ghasemi-Mobarakeh et al., 2008).

Many of the biomaterials in use as ocular devices have been evaluated through various methodological studies using in vitro cell cultures and in vivo animal models. In this study, the in vivo biocompatibility of the PCL nanofiber was investigated inserting this nanostructured material into the vitreous cavity of rat's eye; and evaluating the formation of an inflammatory response. The inflammation is characterized by various important events includ- ing the recruitment of inflammatory cells as well as the injury- induced degranulation of resident mast cells. Then, local immune cells, including resident macrophages, are activated by proin- flammatory mediators released in response to injury. In response to these many signals, the levels of leukocyte chemoattractants increase substantially, further enhancing leukocyte recruitment to the tissue. The neutrophils are the dominant leukocyte in the earliest stages of the inflammatory response. Concomitantly with the influx of neutrophils, circulating monocytes enter the wound and differentiate into mature tissue macrophages (Koh and DiPietro, 2011). If the inflammation does not resolve, the number of inflammatory cells increases, promoting severe damages to the affected tissue. The histological assessment of the ocular tissues after exposition to the PCL nanofiber and its degradation products demonstrated that they did not elicit an inflammatory reaction, since infiltrated inflammatory cells were not observed, and vitr- eous and/or choroidal hemorrhage and retinal detachment were not detected, resulting in the preservation of the integrity of the sensible visual structures of the posterior segment of the eye. The obtained results were similar of those previously described by Bernards and co-workers (Bernards et al., 2013), who demon- strated that micro and nanostructured PCL thin films exhibited acceptable ocular tolerance, once histological evaluation showed no inflammation or morphologic abnormalities at the ocular sites, including the cornea and anterior segment, trabecular meshwork, retina, uvea and vitreous. The limitation of this study was the incomplete physical degradation of the micro and nano polymeric devices during the 6-month implantation period with minimal gross breakdown observed ophthalmoscopically.

The OCT images can identify and quantify the retinal and chor- oidal thickness changes in vivo without enucleation. The existence of an intraocular inflammation resulted from a toxic effect of a bio- material could be clearly detected by the OCT images as a signifi- cant modification in retinal and choroidal thickness (Hwang et al., 2013). In this study, the OCT examination demonstrated that the PCL nanofibers did not provoke an inflammatory reaction and the thickness of the retina and choroid were comparable to the thickness of those structures in the eyes of the animals of the con- trol group. Considering that the architecture of the retina was pre- served, it could be suggested that there was no photoreceptor degeneration caused by disruption of the RPE cells. Therefore, the retinal layers were not atrophic in the presence of the nanostruc- tured fibers, indicating no neuroretinal toxicity. Our OCT results were equivalent of those obtained by Hwang and co-workers (Hwang et al., 2013), who showed that a newly synthesized biodegradable andthermo-sensitive triblock copolymer consisting ofpoly(2-ethyl-2-oxazoline) (PEOz) and poly(ɛ-caprolactone) (PCL) segments (PEOz-PCL-PEOz, ECE), injected into the vitreous cavity of rabbit's eye, did not induce neuroretinal toxicity, demon- strating its ocular safety.

As described above, the inflammatory response within the eye involve the activation of resident macrophages and the recruit- ment of them and other inflammatory cells. Following activation,pro-inflammatory macrophages themselves produce a large number of mediators and cytokines including IL-1, IL-6, IL-12, TNF-a,and iNOS (Koh and DiPietro, 2011). Furthermore, in the injured regions of the eye, the activation and recruitment of micro- glial cells also occur, which damage the photoreceptors of the retina, probably through their secretion of pro-inflammatory mediators and cytotoxic factors, such as TNF-a, IL-1b and nitric oxide (Rutar et al., 2012). Therefore, the existence of an expressive number of activated macrophages and microglia within the eye after the implantation of the PCL nanofibers could represent the installation of an inflammatory reaction in the ocular tissues, and consequently photoreceptor death and local retinal degeneration. However,

the macrophages and microglia stained by IBA-1 were detected in extremely low quantity comparable to the control group, indicating that the nanostructured fibers did not induce an inflammatory response within the eye by activating this kind of cell population.

Besides the activated and recruited macrophages and microglia produce pro-inflammatory cytokines, other retinal cells such as RPE cells are also capable of expressing those cytokines in the injured ocular tissues. The expression of these pro-inflammatory mediators by retinal cells can lead to acute and chronic inflamma- tory processes associated to geographic atrophies inducing retinal degeneration. Therefore, it is mandatory to investigate and quan- tify the production of these substances by the retinal cells and cells from the fundus of the eye exposed to the PCL nanofibers, which could trigger their expression leading to an inflammatory response within the eye. Accordingly to the RT-PCR results, the production of IL-1band iNOS, classic pro-inflammatory cytokines, was extre- mely low for the cells in contact with the nanostructured fibers when compared to the cells non-exposed to the biomaterial. The expression of TNF-afor the retinal cells is also associated to other types of pathophysiological activities including apoptotic cell death, cellular proliferation, differentiation and tumorogenesis. It has been previously reported that TNF-a induction mediated experimental retinal detachment inducing photoreceptor apopto- sis (Ding et al., 2009). Hence, the TNF-a production by the retinal cells was examined following the exposition to the PCL nanofibers; however no significant elevation of the production of the TNF-a was detected. Additionally, the ocular cells did not produce VEGF in a significant manner. It is well documented that the over expres- sion of VEGF is believed to promote the progression of the choroi- dal neovascularization, inducing pathological angiogenesis (Ford and D'Amore, 2012). Finally, the basal level of pro-inflammatory cytokines extracted from the ocular cells of the posterior camera of the eye in contact with the PCL nanofiber indicated that this bio- material did not induce an inflammatory response within the eye, demonstrating its in vivoshort-term biocompatibility.

Finally, the electrospun PCL nanofibers were well tolerated byARPE-19 and MIO-M1 cells, demonstrating no cellular toxic response to the nanostructured mats. These biomaterials were also well tolerated and safety to the delicate tissues of the eye, since they did not elicit an observable cellular infiltration which could result in a severe inflammatory response, culminating in the degeneration of the retinal layers, and consequently, the loss of the visual function. Our excellent in vitro and in vivo results favor its intraocular application as delivery vehicle for controlled release of therapeutic agents to treat the pathologies of the posterior seg- ment of the eye.5. Conclusion

In this work, electrospun PCL nanofiber randomly distributed was developed. The exposition of the polymeric nanostructured material to the ARPE-19 and MIO-M1 cells did not exert cytotoxic effects on the cell phenotype or cell functions, indicating its in vitro biocompatibility. Furthermore, the absence of microglia and macrophage activation, combined with the observed lack of infil- trate inflammatory cells and low expression of cytokines in the ocular tissues suggested that there were no inflammatory response, hemorrhage and neovascularization within the eye exposed to the PCL nanofiber, demonstrating its in vivo biocom- patibility. Considering that the PCL nanofiber did not provide the adhesion ofARPE-19 and MIO-M1 cells due to its hydrophobic sur- face, its applicability as ocular support was compromised. However, as the biocompatibility was demonstrated, it was sug- gested the potential use this biomaterial as a carrier for controlled and prolonged release of the synthetic drogues and bioactive sub- stances aiming the treatment of intraocular diseases.

References

Reneker, D.H., Yarin, A.L., Fong, H., Koombhongse, S., 2000. Bending instability of electrically charged liquid jets of polymer solutions in electrospinning. J. Appl. Phys. 87, 4531–4547.

Ishii, D., Ying, T.H., Yamaoka, T., Iwata, T., 2009. Characterization and biocompatibility of biopolyester nanofibers. Materials 2, 1520–1546.

Moriarty, P., 2001. Nanostructured material. Rep. Prog. Phys. 64 (3), 297–381. Touseef, A., Hassan, M.S., Ba, H.V., Myung-Seob, K., Hak-Kyo, L., Hwang, I.H., 2013. Electrospun Fe$_3$O$_4$/TiO$_2$ hybrid nanofibers and their in vitro biocompatibility: prospective matrix for satellite cell adhesion and cultivation. Mat. Sci. Eng. C 33, 707–713.

Shabani, I., Haddadi-Asl, V., Soleimani, M., Seyedjafari, E., Hashemi, S.M., 2014. Ion- exchange polymer nanofibers for enhanced osteogenic differentiation of stem cells and ectopic bone formation. ACS Appl. Mater. Interfaces 6 (1), 72–82.

Kocabey, S., Ceylan, H., Tekinay, A.B., Guler, M.O., 2013. Glycosaminoglycan mimetic peptide nanofibers promote mineralization by osteogenic cells. Acta Biomater. 9 (11), 9075–9085.

Buchtová, N., Réthoré, G., Boyer, C., Guicheux, J., Rambaud, F., Vallé, K., Belleville, P., Sanchez, C., Chauvet, O., Weiss, P., Le Bideau, J., 2013. Nanocomposite hydrogels for cartilage tissue engineering: mesoporous silica nanofibers interlinked with siloxane derived polysaccharide. J. Mater. Sci. Mater. Med. 24 (8), 1875–1884.

He, X., Fu, W., Feng, B., Wang, H., Liu, Z., Yin, M., Wang, W., Zheng, J., 2013. Electrospun collagen-poly(L-lactic acid-co-e-caprolactone) membranes for cartilage tissue engineering. Regen. Med. 8 (4), 425–436.

Subramanian, A., Krishnan, U.M., Sethuraman, S., 2012. Axially aligned electrically conducting biodegradable nanofibers for neural regeneration. J. Mater. Sci. Mater. Med. 23 (7), 1797–1809.

Du, J., Tan, E., Kim, H.J., Zhang, A., Bhattacharya, R., Yarema, K.J., 2014. Comparative evaluation of chitosan, cellulose acetate, and polyethersulfonenanofiber scaffolds for neural differentiation. Carbohydr. Polym. 99, 483–490.

Wang, F., Li, Z., Guan, J., 2013. Fabrication of mesenchymal stemcells-integrated vascular constructs mimicking multiple properties of the native blood vessels. J. Biomater. Sci. Polym. 24 (7), 769–783.

Huang, N.F., Okogbaa, J., Lee, J.C., Jha, A., Zaitseva, T.S., Paukshto, M.V., Sun, J.S., Punjya, N., Fuller, G.G., Cooke, J.P., 2013. The modulation of endothelial cell morphology, function, and survival using anisotropic nanofibrillar collagen scaffolds. Biomaterials 34 (16), 4038–4047.

Su, Y., Su, Q., Liu, W., Lim, M., Venugopal, J.R., Mo, X., Ramakrishna, S., Al-Deyab, S.S.,El-Newehy, M., 2012. Controlled release of bone morphogenetic protein 2 and dexamethasone loaded in core-shell PLLACL-collagen fibers for use in bone tissue engineering. Acta Biomater 8, 763–771.

Sohrabi, P.M., Shaibani, H., Etayash, K., Kaur, T.T., 2013. Sustained drug release and antibacterial activity of ampicillin incorporated poly(methyl methacrylate)nylon core/shell nanofibers. Polymer 54, 2699–2705.

Chaturvedi, T.P., Srivastava, R., Srivastava, A.K., Gupta, V., Verma, P.K., 2013. Doxycycline poly(e-caprolactone) nanofibers in patients with chronic periodontitis – a clinical evaluation. Methods Mol. Biol. 1014, 187–199.

Liu, J., Liu, J., Xu, H., Zhang, Y., Chu, L., Liu, Q., Song, N., Yang, C., 2014. Novel tumor- targeting, self-assembling peptide nanofiber as a carrier for effective curcumin delivery. Int. J. Nanomed. 9, 197–207.

Son, Y.J., Kim, W.J., Yoo, H.S., 2014. Therapeutic applications of electrospun nanofibers for drug delivery systems. Arch. Pharm. Res. 37, 69–78.

Holan, V., Javorkova, E., Trosan, P., 2013. The growth and delivery of mesenchymal and limbal stem cells using copolymer polyamide 6/12 nanofiber scaffolds. Methods Mol. Biol. 1014, 187–199.

Sharma, S., Mohanty, S., Gupta, D., Jassal, M., Agrawal, A.K., Tandon, R., 2011. Cellular response of limbal epithelial cells on electrospunpoly-e-caprolactone nanofibrous scaffolds for ocular surface bioengineering: a preliminary in vitro study. Mol. Vis. 17, 2898–2910.

Limb, G.A., Salt, T.E., Munro, P.M., Moss, S.E., Khaw, P.T., 2002. In vitro characterization of a spontaneously immortalized human Muller cell line(MIO-M1). Invest. Ophthalmol. Vis. Sci. 43, 864–869.

Fischer, M.D., Huber, G., Beck, S.C., Tanimoto, N., Muehlfriedel, R., Fahl, E., Grimm, C., Wenzel, A., Remé, C.E., Van de Pavert, S.A., Wijnholds, J., Pacal, M., Bremner, R., Seeliger, M.W., 2009. Noninvasive, in vivo assessment of mouse retinal structure using optical coherence tomography. PLoS ONE 4 (10), e7507.

Ouvrard-Pascaud, A., Sainte-Marie, Y., Benitah, J.P., Perrier, R., Soukaseum, C., Cat, A.N., Royer, A., Le Quang, K., Charpentier, F., Demolombe, S.,Mechta-Grigoriou, F., Beggah, A.T., Maison-Blanche, P., Oblin, M.E., Delcayre, C., Fishman, G.I., Farman, N., Escoubet, B., Jaisser, F., 2005. Conditional mineralocorticoid receptor expression in the heart leads tolife-threatening arrhythmias. Circulation 111, 3025–3033.

Silva, G.R., Junior, A.S.C., Saliba, J.B., Berdugo, M., Goldenberg, B.T., Naud, M.C., Ayres, E., Orefice, R.L., Behan-Cohen, F., 2011. Polyurethanes as supports for human retinal pigment epithelium cell growth. Int. J. Artif. Organs 34 (2), 198–209.

Tsukita, S., Oishi, K., Akiyama, T., Yamanashi, Y., Yamamoto, T., 1991. Specific proto- oncogenic tyrosine kinases of src family are enriched incell-to-cell adherens junctions where the level of tyrosine phosphorylation is elevated. J. Cell Biol. 133, 867–879.

Shao-Fen, L., Yu-Xiang, M., Bin, L., Wei, S., Shi-Bo, T., 2013. Morphological and immunocytochemical analysis of human retinal glia subtypes in vitro. Int. J. Ophthalmol. 6 (5), 559–563.

Rutar, M., Natoli, R., Albarracin, R., Valter, K., Provis, J., 2012. 670-nm light treatment reduces complement propagation following retinal degeneration. J. Neuroinflam. 26 (9), 257–267.

Meng, Z.X., Zheng, W., Li, L., Zheng, Y.F., 2010. Fabrication and characterization of three-dimensional nanofiber membrane of PCL-MWCNTsby electrospinning. Mater. Sci. Eng. C 30, 1014–1021.

Lu, J.T., Lee, C.J., Bent, S.F., Fishman, H.A., Sabelman, E.E., 2007. Thin collagen film scaffolds for retinal epithelial cell culture. Biomaterials 28 (8), 1486–1494.

Bringmann, A., Iandiev, I., Pannicke, T., Wurm, A., Hollborn, M., Wiedemann, P., Osborne, N.N., Reichenbach, A., 2009. Cellular signaling and factors involved in Muller cell gliosis: neuroprotective and detrimental effects. Prog. Retin. Eye Res. 28, 423–451.

Kim, J.Y., Cho, D.W., 2009. Blended PCL/PLGA scaffold fabrication usingmulti-head deposition system. Microelectron. Eng. 86, 1447–1450.

Schnell, E., Klinkhammer, K., Balzer, S., Brook, G., Klee, D., Dalton, P., Mey, J., 2007. Guidance of glial cell migration and axonal growth on electrospun nanofibers of poly-e-caprolactone and a collagen/poly-e-caprolactone blend. Biomaterials 28, 3012–3025.

Bakhshandeh, H., Soleimani, M., Hosseini, S.S., Hashemi, H., Shabani, I., Shafiee, A., Nejad, A.H., Erfan, M., Dinarvand, R., Atyabi, F., 2011. Poly (epsilon- caprolactone) nanofibrous ring surrounding a polyvinyl alcohol hydrogel for the development of a biocompatible two-part artificial cornea. Int. J. Nanomed. 6, 1509–1515.

Ghasemi-Mobarakeh, L., Prabhakaran, M.P., Morshed, M., Nasr-Esfahani, M.H., Ramakrishna, S., 2008. Electrospun poly(3-caprolactone)/gelatin nanofibrous scaffolds for nerve tissue engineering. Biomaterials 29, 4532–4539.

Koh, T.J., DiPietro, A.L., 2011. Inflammation and wound healing: the role of the macrophage. Expert. Rev. Mol. Med. 11 (13), e23.

Bernards, D.A., Bhisitkul, R.B., Wynn, P., Steedman, M.R., Lee, O.T., Wong, F., Thoongsuwan, S., Desai, T.A., 2013. Ocular biocompatibility and structural integrity of micro- and nanostructured poly(caprolactone) films. J. Ocular Pharmacol. Therapeut. 29 (2), 249–257.

Hwang, Y.S., Chiang, P.R., Hong, W.H., Chiao, C.C., Chu, I.M., Hsiue, G.H., Shen, C.R., 2013. Study in vivo intraocular biocompatibility of in situ gelation hydrogels: poly(2-ethyloxazoline)-block-poly(e-caprolactone)-block-poly(2-ethyl oxazoline) copolymer, matrigel and pluronic F127. PLoS ONE 1–8 (7), e67495.

Ding, X.Q., Quiambao, A.B., Fitzgerald, J.B., Cooper, M.J., Conley, S.M., Naash, M.I., 2009. Ocular delivery of compacted DNA-nanoparticles does not elicit toxicity in the mouse retina. PLoS ONE 4 (10), e67410.

Ford, K.M., D'Amore, P.A., 2012. Molecular regulation of vascular endothelial growth factor expression in the retinal pigment epithelium. Mol. Vis. 18, 519–527.